Journal of Volcanology and Geothermal Research 326 (2016) 127–142

Contents lists available at ScienceDirect

Journal of Volcanology and Geothermal Research

journal homepage: www.elsevier.com/locate/jvolgeores

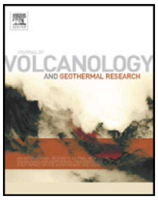

Non-equilibrium processes in ash-laden volcanic plumes: new insights from 3D multiphase flow simulations

Tomaso Esposti Ongaro *, Matteo Cerminara

Istituto Nazionale di Geofisica e Vulcanologia, Sezione di Pisa, Via della Faggiola 32, 56126 Pisa, Italy

ARTICLE INFO

Article history:
Received 1 December 2015
Received in revised form 4 April 2016
Accepted 5 April 2016
Available online 16 April 2016

Keywords:
Explosive eruptions
Turbulent plume
Multiphase flow
Grain-size distribution
Stokes number
Numerical model

ABSTRACT

In the framework of the IAVCEI (International Association of Volcanology and Chemistry of the Earth Interior) initiative on volcanic plume models intercomparison, we discuss three-dimensional numerical simulations performed with the multiphase flow model PDAC (Pyroclastic Dispersal Analysis Code). The model describes the dynamics of volcanic and atmospheric gases (in absence of wind) and two pyroclastic phases by adopting a non-equilibrium Eulerian–Eulerian formulation. Accordingly, gas and particulate phases are treated as interpenetrating fluids, interacting with each other through momentum (drag) and heat exchange. Numerical results describe the time-wise and spatial evolution of weak (mass eruption rate: 1.5×10^6 kg/s) and strong (mass eruption rate: 1.5×10^9 kg/s) plumes. The two tested cases display a remarkably different phenomenology, associated with the different roles of atmospheric stratification, compressibility and mechanism of buoyancy reversal, reflecting in a different structure of the plume, of the turbulent eddies and of the atmospheric circulation. This also brings about different rates of turbulent mixing and atmospheric air entrainment. The adopted multiphase flow model allows to quantify temperature and velocity differences between the gas and particles, including settling, preferential concentration by turbulence and thermal non-equilibrium, as a function of their Stokes number, i.e., the ratio between their kinetic equilibrium time and the characteristic large-eddy turnover time of the turbulent plume. As a result, the spatial and temporal distribution of coarse ash in the atmosphere significantly differs from that of the fine ash, leading to a modification of the plume shape. Finally, three-dimensional numerical results have been averaged in time and across horizontal slices in order to obtain a one-dimensional picture of the plume in a stationary regime. For the weak plume, the results are consistent with one-dimensional models, at least in the buoyant plume region, and allow to reckon a variable, effective entrainment coefficient with a mean value around 0.1 (consistently with laboratory experiments). For the strong plume, analysis of the results reveals that the two most critical assumptions of one-dimensional integral models are the self-similarity and the pressure equilibrium. In such a case, the plume appears to be controlled by the dynamics in the jet stage (below the buoyancy reversal) and by mesoscale vorticity associated with the development of the umbrella.

1. Introduction

The dynamics of volcanic plumes have received a renewed attention in the last years because of the recognition of their importance for the accurate prediction of the ash dispersal by wind and its related hazard for the aviation (e.g. Mastin et al., 2009; Guffanti and Tupper, 2015). In particular, because the wind strength and direction can be non-homogeneous in height (especially crossing the tropopause), the vertical mass distribution of the pyroclastic and gaseous components in the plume can have a significant impact on the forecast of ash dispersal by advection–diffusion models.

To address this problem, one-dimensional integral plume models including the effect of wind (e.g., Bursik, 2001; Folch et al., 2016) and atmospheric conditions (e.g., Glaze and Baloga, 1996) have been developed based on the pioneering works by Morton et al. (1956), Morton (1959), Wilson et al. (1978, 1980), Woods (1988). Such integral models have had a formidable role in correlating the (observed or reconstructed) maximum plume height to the mass eruption rate, thus posing new fundamental constrains on the characterization of explosive eruptions on the basis of their intensity. The most recent studies (Ishimine, 2006; Scase, 2009; Woodhouse et al., 2013; de' Michieli Vitturi et al., 2015; Cerminara et al., 2015, among others) have provided further constraints to the interpretation of geophysical observations and sedimentological data.

At the same time, numerical models of volcanic plumes have been developed to get new insight into the complex, three-dimensional and multiphase nature of volcanic plumes (Oberhuber et al., 1998; Neri et al., 2003; Suzuki et al., 2005; Esposti Ongaro et al., 2008; Cerminara et al., 2016a), to explore the influence of more realstic vent conditions and to put further constraints on semi-empirical parameters needed by integral models, in particular, the entrainment coefficient (Suzuki

---

* Corresponding author.
E-mail address: tomaso.espostiongaro@ingv.it (T. Esposti Ongaro).

http://dx.doi.org/10.1016/j.jvolgeores.2016.04.004

and Koyaguchi, 2010), also in presence of wind (Suzuki and Koyaguchi, 2015; Van Eaton et al., 2015). Nonetheless, despite the early identification of relevant non-equilibrium effects on volcanic columns (e.g., Valentine and Wohletz, 1989; Dobran et al., 1993) and the recognition that equilibrium assumption is valid only on a restrict range of particle sizes, the non-equilibrium dynamics in volcanic plumes have never been addressed specifically.

In the framework of the IAVCEI (International Association of Volcanology and Chemistry of the Earth Interior) initiative on volcanic plume models intercomparison (Costa et al., 2016; Suzuki et al., 2016b), in this paper we use the three-dimensional numerical flow model PDAC (Section 3) to investigate the non-equilibrium effects in volcanic plumes, focussing on the windless case. Numerical model results presented in Section 4 allow to analyse the different behaviour of two particle classes (representative of fine and coarse ash) and their influence on the large-scale plume dynamics. Model results are then integrated in time and space to obtain a one-dimensional picture of the plume, and results are interpreted in the light of elementary scaling analysis (Section 5). In Section 6, we analyse the main hypotheses of one-dimensional integral models, namely: 1) the self-similarity of the velocity and temperature profiles; 2) stationary flow; 3) pressure equilibrium along horizontal sections; 4) entrainment hypothesis, on the basis of three-dimensional results. We finally (Section 7) frame the present work in the context of the inter-comparison study and address some ideas for future works.

2. Eruptive scenarios: weak and strong plumes

The set of input data for the complete model inter-comparison research is discussed in the companion paper by Costa et al. (2016). In this work, we have limited our analysis on the windless scenarios for a weak (WP) and a strong (SP) plume, focussing our attention on the non-equilibrium multiphase effects and on the multidimensional plume behaviour. Although the definition of weak and strong plume is usually associated with the relative strength of the updraught with respect to the wind speed, we will show in Section 6 that it is worth maintaining the distinction even in the windless case, basing upon their different scaling properties. This point is also discussed by Costa et al. (2016) and Suzuki et al. (2016b), and it is the main topic of Suzuki et al. (2016a).

In the WP case, the mass flow rate is 1.5×10^6 kg/s (a small-moderate eruption, accordingly to Bonadonna and Costa (2013), whereas in the SP case the mass flow rate is 1.5×10^9 kg/s (a Plinian eruption, Newhall and Self, 1982). Although not explicitly specified during the exercise, the weak plume scenario was based on the 26 January 2011 Shinmoe-dake eruption (e.g., Hashimoto et al., 2012; Kozono et al., 2013; Suzuki and Koyaguchi, 2013). The strong plume scenario was based on the climactic phase of the Pinatubo eruption, Philippines, on 15 June 1991 (e.g. Holasek et al., 1996; Costa et al., 2013). For both scenarios, only two particle size classes were considered, representing coarse ash and fine ash, each comprising 50 wt.% of the erupted solid mass. The corresponding vent conditions for WP and SP are reported in Table 1.

2.1. Atmospheric conditions

The input conditions describe injection of the eruptive mixture from a vent (without a crater) into a stably stratified atmospheric profile with $P = P_{1500}, T = T_{1500}$ at the vent level ($z = 1500$ m) and a thermal vertical gradient as specified in the benchmark case. To build a stable atmospheric profile, we imposed the pressure P_0 and temperature T_0 at the sea level, the height and the thermal gradients in the atmospheric layers as reported in Table 2 and computed the density and pressure profiles by imposing the hydrostatic equilibrium. No humidity profile was imposed in the initial atmosphere.

Table 1
Numerical vent conditions for the weak and strong plumes. Notation: M_f mass flow rate, D vent diameter, P pressure, T temperature, ρ density, w vertical component of the velocity, d particle diameter, ε volumetric fraction. Subscrit g indicates the gas phase, $s1$ and $s2$ the coarse and fine ash, respectively.

Vent parameter	WP	SP	Units
D	54	1417	m
w_g	135	275	m/s
P_g	85,215	85,656	Pa
T_g	1273	1053	K
ρ_g	0.145	0.175	kg/m ^{3}
w_{s1}, w_{s2}	135	275	m/s
T_{s1}, T_{s2}	1273	1053	K
ρ_m	4.688	3.285	kg/m ^{3}
M_f	$1.5 \cdot 10^6$	$1.5 \cdot 10^9$	kg/s
d_{s1}	1.0	0.5	mm
ρ_{s1}	2200	2500	kg/m ^{3}
ε_{s1}	0.00106553	0.0006574	
d_{s2}	0.0625	0.016	mm
ρ_{s2}	2700	2700	kg/m ^{3}
ε_{s2}	0.00086821	0.0006087	

3. Fluid-dynamic model

To describe the spatio-temporal evolution of the two eruptive scenarios, in this work we adopt a transient, three-dimensional, non-equilibrium multiphase flow model (Neri et al., 2003; Esposti Ongaro et al., 2007). To describe the bi-disperse gas–particle mixture, the gas and each particle class are described as continuum fluid phases in a field (Eulerian–Eulerian) approach. Accordingly, at each point of the domain we define, for gas (subscript g) and the two solid phases ($s1, s2$), the bulk density $\tilde{\rho}$, momentum $\tilde{\rho}\mathbf{u}$ and enthalpy $\tilde{\rho}h$ per unit of volume, where the bulk density is the mass of the given phase per unit of volume. The bulk density can be expressed as $\tilde{\rho} = \varepsilon\rho$, where ε is the fraction of the volume occupied by the phase and ρ is the thermodynamic density, which is constant for the solid phases and depends on pressure and temperature through the equation of state $\rho_g = \rho_g(P,T)$ for the gas phase. Conservation of mass, momentum and energy in an arbitrary volume allow to write a set of partial differential equations describing the evolution of the Eulerian fields in time, from a prescribed set of initial and boundary conditions. Model equations are reported synthetically in Appendix A.1.

In this description, the gas and particulate phases in the plume can have different velocities and temperatures, because of different injection regimes or because they are subject to different forces (such as the effective gravity, or buoyancy), while drag forces and heat exchange will tend to homogeneize the flow. Therefore, the description of

Table 2
Physical parameters characterizing the initial atmospheric stratification in the WP and SP cases.

Parameter	WP	SP	Units
P_0 ($z = 0$ m)	102,700	101,325	Pa
T_0 ($z = 0$ m)	282.84	299.83	K
P_{1500} ($z = 1500$ m)	85,215	85,656	Pa
T_{1500} ($z = 1500$ m)	274.23	289.84	K
Troposphere (TS)	17.0	16.0	km
Tropopause (TP)	20.0	17.0	km
Lower stratosphere (LS)	–	21.0	km
Upper stratosphere (US)	–	47.0	km
Stratopause (SP)	–	51.0	km
Lower mesosphere (LM)	–	71.0	km
∇T_{TS}	-5.74	-6.66	K/km
∇T_{TP}	0.0	-1.0	K/km
∇T_{LS}	–	$+4.0$	K/km
∇T_{US}	–	$+2.4$	K/km
∇T_{SP}	–	0.0	K/km
∇T_{LM}	–	-2.8	K/km